Modeling and Discretization of Hydraulic Actuated Telescopic Boom System in Port-Hamiltonian Formulation

Lingchong Gao[1], Wang Mei[2], Michael Kleeberger[1], Haijun Peng[3] and Johannes Fottner[1]
[1]*Chair of Materials Handling, Material Flow, Logistics, Technical University of Munich, Botlzmannstrasse15, 85748 Garching, Germany*
[2]*Chair of Automatic Control, Technical University of Munich, Botlzmannstrasse15, 85748 Garching, Germany*
[3]*Department of Engineering Mechanics, Dalian University of Technology, Linggong Road No. 1, 116023 Dalian, P.R. China*
{*lingchong.gao, michael.kleeberger, j.fottner*}*@tum.de, mei.wang@tum.de, hjpeng@dlut.edu.cn*

Keywords: Port-Hamiltonian System, Structure-preserving Discretization, Hydraulic Cylinder, Telescopic boom.

Abstract: The hydraulic actuated telescopic boom system is the primary operation actuator of mobile cranes and aerial platform vehicles. The purpose of this paper is to develope a unified mathematic model of such a boom system which is a multi-domain system consisting of boom structure and hydraulic drive system. The model is formulated within the port-Hamilton (PH) formalism using the definition of hydraulic system and elastic boom structure as (Stokes-) Dirac structures. The Port-Hamiltonian systems can be easily interconnected thus allowing the description of a complex system as a composition of subsystems. This property is especially useful to model a multi-domain system with energy exchanges between subsystems. Considering the boom structure as a Timoshenko beam, the luffing operation of boom system is simplified in a plane coordinate system. The Port-Hamiltonian model of the hydraulic system and the boom structure are described with details separately, a structure-preserving discretization is applied to transfer the distributed-parameter boom model into a lumped-parameter model. Then the interconnections between the subsystems are illustrated and a complete simulation including hydraulic system is accomplished in MATLAB/Simulink.

1 INTRODUCTION

Mobile cranes and aerial platform vehicles are construction machineries designed to lift heavy loads for construction operations and to assist high altitude operations respectively. They are generally equipped with long boom systems. The boom system can be considered as a long boom manipulator that consists of single or multiple long and lightweight booms, using hydraulic actuators along with an electro-hydraulic servo system to control the movements. Because of its high energy density, the hydraulic system is suitable to actuate such large scale boom systems with heavy loads. Due to the long boom system, mobile cranes are suitable for lifting tasks with large radius and height, whereas aerial platform vehicle can transport persons and equipment to high operation positions for installation, maintenance or fire rescue missions. The longest boom system of mobile cranes has reached the length of 250 meter and the highest position that can be reached by aerial platform vehicles is 114 meter.

In order to reduce the self-weight and to ensure the mobility as well as transport-ability, the boom systems of mobile cranes and aerial platform vehicles are designed as light as possible. The boom structures with limited stiffness are always performing a strong flexible behavior, even though the strength of the boom system is ensured. Due to the dynamic behavior of hydraulic actuators (hydraulic cylinders or motors) which derives from the elastic hydraulic oil and flow characteristics of hydraulic components, the output of the hydraulic system during start-up and braking stages of the operations could fluctuate significantly. The combination of the elastic drive system and the flexible boom structure leads to a hybrid system with complex dynamic behavior. The flexibility of the boom structure can cause an intense vibration response when the loads applied on the boom structure or the motion statuses of boom system change. The structure vibration will increase the maximum dynamic stress which could cause structure fatigue or even structure failure. The oscillation at the boom's tip could also increase the difficulty of load locat-

Gao, L., Mei, W., Kleeberger, M., Peng, H. and Fottner, J.
Modeling and Discretization of Hydraulic Actuated Telescopic Boom System in Port-Hamiltonian Formulation.
In *Proceedings of the 9th International Conference on Simulation and Modeling Methodologies, Technologies and Applications (SIMULTECH 2019)*, pages 69-79
ISBN: 978-989-758-381-0

ing or endanger the safety of the personnel on platforms. The vibration suppression for these large scale boom systems is essential for improving the structure fatigue life-cycle, operation efficiency and personnel safety.

Some researchers focus on the dynamic analysis of the boom structure, some others have investigated the analysis of the whole boom system including hydraulic system and use hydraulic actuators to control the structure vibration. Sun combined the finite element calculation method with mathematical formulations of hydraulic drive system including essential hydraulic components, to obtain a new model which describes the dynamic interaction between the boom structure and the drive system of mobile crane. (Sun and Kleeberger, 2003). The method has been applied for the exemplary calculation of slewing, lifting and luffing operations of lattice boom cranes (Sun et al., 2005)(Sun and Liu, 2006). Both the load-bearing structure and the drive system can be described in details. The calculation of a telescopic boom crane has also been studied. Similar long boom systems are also used in fire-rescue turntable ladders. The boom system of a fire-rescue turntable ladder is a telescopic lattice boom actuated by a hydraulic cylinder. Sawodny described the long fire-rescue turntable ladder as a flexible multi-body system (Zuyev and Sawodny, 2005) and the dynamic behavior of the hydraulic drive system was included in the mathematical model equations (Sawodny et al., 2002). In the work of Pertsch (Pertsch et al., 2009), a distributed-parameter model for the fire-rescue turntable ladder was derived, based on the Euler-Bernoulli beam theory. The model of the ladder structure was transferred into low dimensional model space. In their recent work (Pertsch and Sawodny, 2016), a model for the coupled bending-torsional vibration associated with the rotational motion of an articulated aerial ladder has been derived and an active vibration damping control has been developed and validated in real operation.

The hydraulic actuated telescopic boom can be regarded as a multi-physical system consisting of the mechanical structure, hydraulic drives and electrical control system. The interconnections between the subsystems are achieved by hydraulic actuators and electro-hydraulic servo systems. With the increasing demands for more accurate control precision during the operations of these long boom manipulators, the dynamic analysis for such multi-physical systems has been extended from the dynamic respond study of separated subsystems to a coupling analysis of different domain subsystems. The bond-graph method (Gawthrop and Bevan, 2007) is a graphical approach in which the component energy ports are connected by bonds using power-conjugate variables, efforts and flows, to illustrate the energy transformation and conversion between components and different physical systems. This port-based modeling method is widely used to build a mathematical model of electromechanical multi-domain systems (Guo et al., 2016) (Cheng et al., 2016). The representation of a physical system as a bond graph can lead to a dynamical system endowed with a geometric structure, which is called a Port-Hamiltonian (PH) system. The geometric structure called Dirac structure is introduced as the key mathematical concept to unify the description of complex interactions in multi-physical systems. The Hamiltonian function of the system energy which is used to derive system state space equations, can also be used as Lyapunov function for stability analysis.

Many researchers did a lot of work on the system modeling and control design for flexible beam systems based on their representation as Port-Hamiltonian system. Macchelli also reformulated the Timoshenko model of beam within the framework of the Port-Hamiltonian system (Macchelli and Melchiorri, 2004). The transitional and rotational deflections and momenta were chosen as state variables to build the (Stokes-) Dirac structure. He also used Port-Hamiltonian approach to describe the multi-body system (rigid body, flexible links and kinematic pairs) based on the power conserving interconnection (Macchelli et al., 2009). In order to solve the infinite dimensional model in Port-Hamiltonian formulation, a structure-preserving discretization method is needed. So that the discretized finite-dimensional model still has the property of (Stokes-) Dirac structure (Moulla et al., 2012)(Vu et al., 2013). Wang applied a geometric pseudo-spectral discretization to obtain the finite-dimensional Port-Hamiltonian framework of linear Timoshenko beam model, and solved the feed-forward motion control problem based on this lumped model (Wang et al., 2017). For the hydraulic systems, Kugi designed a nonlinear controller for a classical hydraulic piston actuator system based on the Port-Hamiltonian model (Kugi and Kemmetmüller, 2004). In his doctor thesis (Stadlmayr, 2009), Stadlmayr gave a Port-Hamiltonian representation of flexible manipulator consisting a long boom with a mass at the tip and a hydraulic system using hydraulic cylinder to actuate the manipulator (Stadlmayr and Schlacher, 2004). Combined with feed-forward and feedback control system, a MIMO-control was designed and used to accomplish path tracking and vibration suppression for the flexible manipulator.

2 SYSTEM DESCRIPTION

2.1 Port-Hamiltonian System

From the above research, it has shown that the Port-Hamiltonian framework is a proper modeling method for multi-domain systems because of its unique mathematical structure. To definite a Port-Hamiltonian system, we start with the definition of a suitable space of power variables which are strictly related to the geometry structure of the system. A Dirac structure defined on this space of power variables will be used to describe the internal and external interconnection of the system. We consider a linear space $\mathscr{F}$ (space of generalized velocities or flows) and its dual denotes as $\mathscr{E} = \mathscr{F}^*$ (space of generalized forces or efforts). The space of the power variables is $\mathscr{F} * \mathscr{E}$. According to the definition given by Duidam (Duindam et al., 2009), there exists a canonically defined symmetric bilinear form on $\mathscr{F} * \mathscr{E}$

$$\ll (f_1, e_1), (f_2, e_2) \gg := \langle e_1 \,|\, f_2 \rangle + \langle e_2 \,|\, f_1 \rangle, \qquad (1)$$

where $f_i \subset \mathscr{F}$, $e_i \subset \mathscr{E}$ and $\ll ., . \gg$ denotes the duality product between $\mathscr{F}$ and its dual space $\mathscr{E}$. A constant Dirac structure on $\mathscr{F}$ is a linear subspace $\mathscr{D} \subset \mathscr{F} \times \mathscr{E}$ with the property $\mathscr{D} = \mathscr{D}^{\perp}$. A crucial property of the Dirac structure is that the standard interconnection of Dirac structures is again a Dirac structure (Duindam et al., 2009). Thus the components of each system will be described as energy-storing elements, resistive elements with the formation of Dirac structure and also called as internal ports. The energy exchanges between the system and environment (other systems) are described by external ports, interaction ports and control ports specifically. So that the system consisting of these components is still a Dirac structure, so as a large-scale multi-domain system composed of multiple subsystems which have the formulations of Dirac structure.

The system energy function Hamiltonian $H(x)$ is used to build the mathematical model of the system. The state space variables x reflect the system flow variables by the definition of $\dot{x} = f$ and the system effort variables e are given by the co-energy variables $\partial H(x)/\partial x$. All the subsystems can be described in the form of

$$\begin{aligned} \dot{x} &= (\boldsymbol{J}(x) - \boldsymbol{R}(x))(\frac{\partial H}{\partial x}(x))^{\top} + \boldsymbol{G}(x)u \\ y &= \boldsymbol{G}(x)(\frac{\partial H}{\partial x}(x))^{\top} \end{aligned} \qquad (2)$$

which is a useful formulation because the matrix $\boldsymbol{J}(x)$ is a skew-symmetric matrix and the components of $\boldsymbol{J}(x)$ are smooth functions of the state variables. The matrix $\boldsymbol{R}$ has to be symmetric and positive semi-definite $\boldsymbol{R} = \boldsymbol{R}^{\top} \geq 0$. A dynamic system with such formation is called a Port-Hamiltonian system. In order to model the whole boom system as Port-Hamiltonian system, the space of power variables of hydraulic system and boom structure will be defined with numerical Dirac structure. The representation of the boom system is written as the combination of the hydraulic system and the boom structure in the formulations of a Port-Hamiltonian system. For the sake of simplicity, the damping effect is momentarily neglected in the following chapters.

2.2 Port-Hamiltonian Model of Hydraulic System

2.2.1 Essential Equations and Assumptions

The luffing cylinder of the boom system can be simply considered as the hydraulic cylinder actuator of Fig. (1). A 4/3-way proportional directional valve controls the movement of the asymmetric cylinder, which actuates the luffing movement of the boom system. The directional valve is connected with a pressure pump and a tank. The supply pressure p_{S} is determined by the relief valve, and the tank pressure is p_{T}.

The volumetric flows through the directional valve, Q_1 and Q_2, are simply given by

$$Q_i = k_{\mathrm{v}} \sqrt{\Delta p_i} x_{\mathrm{v}}, i = 1, 2 \qquad (3)$$

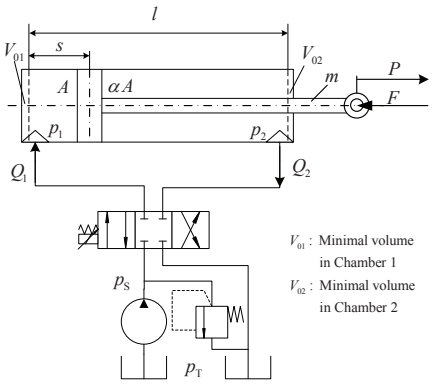

Figure 1: Diagram of the hydraulic system of a hydraulic cylinder.

with the position of the valve core x_{v}, the pressure difference Δp_i and the valve coefficient k_{v}, which can be considered as constant when the properties of the flow through the valve ports are constant and the type of valve core is slide valve. Then, we assume that there is no internal or external leakage flows and the temperature remains constant. The continuity equations

of the cylinder chambers can be described as

$$\frac{\mathrm{d}}{\mathrm{d}t}(As) = Q_1, \frac{\mathrm{d}}{\mathrm{d}t}(\alpha A(l-s)) = Q_2. \tag{4}$$

Using the linearized constitutive law of the constant (isothermal) bulk modulus E_{oil}

$$E_{\text{oil}} = \rho \frac{\partial p}{\partial \rho}, \tag{5}$$

we can rewrite Eq. (3) as a well-known formation

$$\begin{aligned} \dot{p}_1 &= \frac{E_{\text{oil}}}{V_{01} + As} \left(-A\frac{P}{m} + Q_1 \right) \\ \dot{p}_2 &= \frac{E_{\text{oil}}}{V_{02} + \alpha A(l-s)} \left(\alpha A \frac{P}{m} - Q_2 \right) \end{aligned} \tag{6}$$

with the piston's momentum P and its mass m. And the motion equations of the piston are considered as the following form

$$\begin{aligned} \dot{S} &= \frac{P}{m} \\ \dot{P} &= (p_1 A - p_2 \alpha A - F). \end{aligned} \tag{7}$$

Eq. (7) and (6) constitute a state model of the valve-controlled hydraulic cylinder of Fig. (1) with the state vector $\boldsymbol{x} = [s, P, p_1, p_2]^\top$.

2.2.2 Energy Description of Isentropic Fluid

In the case of an isentropic process no heat transfer between the environment and the considering system, which performs only work of expansion. The system energy can be simplified as

$$\mathrm{d}U = -p\mathrm{d}V. \tag{8}$$

By defining the specific internal energy $u = U/M$ and the specific volume $v = V/M$, with M the mass of the fluid in the system, we can get

$$\mathrm{d}u = -p\mathrm{d}v = \frac{p}{\rho^2}\mathrm{d}\rho \tag{9}$$

where $\rho = 1/v$ is the density of the fluid.

Now we introduce another important thermodynamic quantity, the enthalpy $H = U + pV$ and the mass specific enthalpy $h = H/M = u + pv$. Combining the definition of h with (9), we get the following relations for the isentropic scenario

$$h = u + \frac{1}{\rho}p = u + \frac{1}{\rho}\rho^2 \frac{\partial u}{\partial \rho} = \frac{\partial}{\partial \rho}(u\rho) \tag{10}$$

Based on the definition of isothermal bulk modules, integrating along an isentropic process, Eq. (5) yields

$$p(\rho) = p_0 + E_{\text{oil}} \ln\left(\frac{\rho}{\rho_0}\right) \text{ with } p_0 = p(\rho_0). \tag{11}$$

Then, the specific energy of the fluid obeying the constitutive law (5) can be obtained form (9) in the form:

$$\begin{aligned} u(p) &= \frac{\left(p_0 + E_{\text{oil}} + u_0\rho_0 - (p + E_{\text{oil}})e^{((p_0-p)/E_{\text{oil}})}\right)}{\rho_0} \\ &\text{with } u_0 = u(p_0). \end{aligned} \tag{12}$$

For the sake of convenience we will subsequently choose $p_0 = 0$ and $u_0 = 0$. Hence the internal energy results in

$$U(p) = \overbrace{V\rho(p)}^{M} u(p) = V\left(E_{\text{oil}}\left(e^{(p/E_{\text{oil}})} - 1\right) - p\right). \tag{13}$$

Using the above formulation, we can acquire the energy function of the fluid inside the hydraulic cylinder, which is essential to building the Hamiltonian function of the system.

2.2.3 Port-Hamiltonian Representation of Hydraulic Cylinder

The specific internal energy $u(p)$ of the fluid in the two chambers of the hydraulic cylinder can be determined by (12), then the energy stored in the hydraulic cylinder of Fig. 1 is given by

$$\begin{aligned} U_{\text{Hydr}} &= V_1\rho_1 u(p_1) + V_2\rho_2 u(p_2) \\ &= E_{\text{oil}} \sum_{i=1,2} V_i \left(e^{(p_i/E_{\text{oli}})} - \frac{p_i}{E_{\text{oil}}} - 1 \right) \\ V_1 &= V_{01} + As, V_2 = V_{02} + \alpha A(l-s), \end{aligned} \tag{14}$$

the subscripts refer to the corresponding quantities of the chamber 1 and chamber 2 (rob side). Assuming that the kinetic energy of fluid mass can be neglected compared to the kinetic energy of the piston, the total energy E_{c} of the hydraulic cylinder is

$$E_{\text{c}} = U_{\text{Hyd}} + \frac{P^2}{2m}. \tag{15}$$

We can use the total energy E_{c} as the Hamiltonian function H_{c}, then the Port-Hamiltonian model of the hydraulic cylinder takes the form as (2) with the state vector $\boldsymbol{x} = [s, P, p_1, p_2]^\top$ and the input vector $\boldsymbol{u} = [F, Q_1, Q_2]^\top$, the hydraulic cylinder can be described as $\sum_0$

$$\Sigma_0 : \begin{cases} \dot{\boldsymbol{x}} = \boldsymbol{J}(x)\partial_x H_{\text{c}} + \boldsymbol{g}(x)\boldsymbol{u} \\ \boldsymbol{y} = \boldsymbol{g}(x)^\top \partial_x H_{\text{c}} \end{cases} \tag{16}$$

The matrices $\boldsymbol{J}(x)$ and $\boldsymbol{g}(x)$ are

$$\boldsymbol{J}(x) = \begin{bmatrix} 0 & 1 & 0 & 0 \\ -1 & 0 & E_{\text{oil}}A/V_1 & -E_{\text{oil}}\alpha A/V_2 \\ 0 & -E_{\text{oil}}A/V_1 & 0 & 0 \\ 0 & E_{\text{oil}}\alpha A/V_2 & 0 & 0 \end{bmatrix} \tag{17}$$

$$\boldsymbol{g}(x) = \begin{bmatrix} 0 & 0 & 0 \\ -1 & 0 & 0 \\ 0 & E_{\text{oil}}/V_1 & 0 \\ 0 & 0 & -E_{\text{oil}}/V_2 \end{bmatrix} \tag{18}$$

In order to illustrate the system output $\boldsymbol{y}$, more details of the model is given by

$$\frac{\partial H_{\text{c}}}{\partial x} = \begin{bmatrix} \alpha A(\Gamma_2) - A(\Gamma_2) \\ P/m \\ V_1\left(e^{(p_1/E_{\text{oil}})} - 1\right) \\ V_2\left(e^{(p_2/E_{\text{oil}})} - 1\right) \end{bmatrix}, \tag{19}$$

with $\Gamma_i = p_i - E_{\text{oil}}\, e^{(p_i/E_{\text{oil}})} + E_{\text{oil}}, i = 1,2.$

Then using the definition (13), the system output is

$$\begin{aligned} \boldsymbol{y} &= \boldsymbol{g}(x)^\top \frac{\partial H_{\text{c}}}{\partial x} \\ &= \begin{bmatrix} 0 & -1 & 0 & 0 \\ 0 & 0 & E_{\text{oil}}/V_1 & 0 \\ 0 & 0 & 0 & -E_{\text{oil}}/V_2 \end{bmatrix} \frac{\partial H_{\text{c}}}{\partial x} \\ &= \begin{bmatrix} -p/m \\ E_{\text{oil}}\left(e^{(p_1/E_{\text{oil}})} - 1\right) \\ -E_{\text{oil}}\left(e^{(p_2/E_{\text{oil}})} - 1\right) \end{bmatrix} = \begin{bmatrix} -v \\ \rho_1 h_1 \\ -\rho_2 h_2 \end{bmatrix} \end{aligned} \tag{20}$$

The change of the system energy can be obtained by the product of input $\boldsymbol{u}$ and output $\boldsymbol{y}$ as

$$\frac{\mathrm{d}E_{\text{c}}}{\mathrm{d}t} = \boldsymbol{y}^\top \boldsymbol{u} = h_1 \underbrace{\rho_1 Q_1}_{\dot{M}_1} - h_2 \underbrace{\rho_2 Q_2}_{\dot{M}_2} - v \cdot F \tag{21}$$

In Eq. (21), the first two parts represent the energy changed by the fluid mass flows to or from the chambers respectively, $\dot{M}_1$ or $\dot{M}_2$, and the third part represents the work transferred to the boom structure by cylinder force F.

2.3 Port-Hamiltonian Model of 2-D Timoshenko Beam

2.3.1 A Rotation Homogeneous Timoshenko Beam

The boom structure can be simplified as an ideal beam model in a plane, when the lateral and axial loads can be neglected. In order to obtain a suitable Port-Hamiltonian representation of the boom structure, we start with the rotating homogeneous Timoshenko beam formulation to describe the dynamic behavior of the boom structure.

In Fig. 2. , t is the time variable and z is the spatial coordinate along the equilibrium position of the beam, and $w_{\text{e}}(z,t)$ is the deflection of the beam from

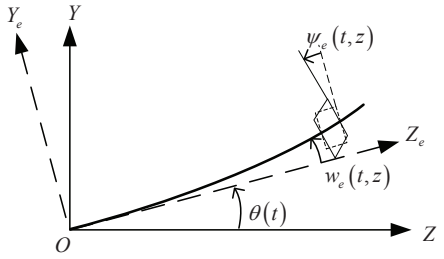

Figure 2: A rotation homogeneous Timoshenko beam.

the equilibrium position and $\Psi_{\text{e}}(z,t)$ is the rotation of the beam's cross section.

The boundary condition of the boom structure can be considered as a free tip with a fixed end, and the fixed end rotates around a fixed axis with the angle displacement $\theta(t)$. Then the original Timoshenko beam model is transferred to a rotating Timoshenko beam. New system variables are defined as

$$\begin{aligned} w(z,t) &= w_e(z,t) + z \cdot \theta(t) \\ \psi(z,t) &= \psi_e(z,t) + \theta(t) \end{aligned} \tag{22}$$

which still fulfill the original PDEs in a new form

$$\begin{aligned} &\rho \frac{\partial^2 w}{\partial t^2} - K\frac{\partial^2 w}{\partial z^2} + K\frac{\partial \psi}{\partial z} = 0 \\ &I_\rho \frac{\partial^2 \psi}{\partial t^2} - EI\frac{\partial^2 \psi}{\partial z^2} + K\left(\psi - \frac{\partial w}{\partial z}\right) = 0 \end{aligned} \tag{23}$$

In (23), the coefficients ρ, I_ρ, E, I are the mass per unit length, the mass moment of inertia of the cross section, Young's modulus and the moment of the inertia of the cross section respectively. And in the coefficient $K = kGA$, G is the modulus of elasticity in shear, A is the area of cross section and k is a constant depending on the shape of the cross section.

2.3.2 Port-Hamiltonian Model of Timoshenko Beam

For a homogeneous Timoshenko beam, the coefficients are constant and its mechanical energy is given as following form:

$$\begin{aligned} H_{\text{B}}(t) &= \int_0^L H \mathrm{d}z \\ H &= \frac{1}{2}\left(\rho \dot{w}^2 + I_\rho \dot{\psi}^2 + K(\psi - \partial_z w)^2 + EI(\partial_z \psi)^2\right). \end{aligned} \tag{24}$$

According to the mechanical energy formulation (24) the potential elastic energy is the function of the shear and bending deformations, which can be written as:

$$\begin{aligned} \varepsilon_{\text{t}}(z,t) &= \partial_z w(z,t) - \psi(z,t) \\ \varepsilon_{\text{r}}(z,t) &= \partial_z \psi(z,t). \end{aligned} \tag{25}$$

The associated co-energy variables are shear force $K\varepsilon_t(z,t)$ and bending momentum $EI\varepsilon_r(z,t)$. The kinetic energy is the function of the translational and

rotational momenta which are given as

$$\begin{aligned} p_{\mathrm{t}}(z,t) &= \rho \dot{w}(z,t), \\ p_{\mathrm{r}}(z,t) &= I_\rho \dot{\psi}(z,t), \end{aligned} \tag{26}$$

and the co-energy variables are translational velocity $(p_{\mathrm{t}}(z,t))/\rho$ and rotational velocity $p_{\mathrm{r}}(z,t)/I_\rho$.

According to the definition of new state variables, the original PDEs can be rewritten in a form

$$\begin{bmatrix} \dot{p}_{\mathrm{t}} \\ \dot{p}_{\mathrm{r}} \\ \dot{\varepsilon}_{\mathrm{t}} \\ \dot{\varepsilon}_{\mathrm{r}} \end{bmatrix} = \begin{bmatrix} 0 & 0 & \partial_z & 0 \\ 0 & 0 & 1 & \partial_z \\ \partial_z & -1 & 0 & 0 \\ 0 & \partial_z & 0 & 0 \end{bmatrix} \begin{bmatrix} \delta_{p_t} H \\ \delta_{p_r} H \\ \delta_{\varepsilon_t} H \\ \delta_{\varepsilon_r} H \end{bmatrix}. \tag{27}$$

We denote $\boldsymbol{e} \in \mathscr{E}$, $\boldsymbol{f} \in \mathscr{F}$ as the effort and flow variables separately. They are related to the time derivative of state variables $\boldsymbol{f} = -\dot{\boldsymbol{x}}$ and the associated co-energy variables as

$$\boldsymbol{f} = \begin{bmatrix} f^{p_{\mathrm{t}}} \\ f^{p_{\mathrm{r}}} \\ f^{\varepsilon_{\mathrm{t}}} \\ f^{\varepsilon_{\mathrm{r}}} \end{bmatrix} = - \begin{bmatrix} \dot{p}_{\mathrm{t}} \\ \dot{p}_{\mathrm{r}} \\ \dot{\varepsilon}_{\mathrm{t}} \\ \dot{\varepsilon}_{\mathrm{r}} \end{bmatrix}, \boldsymbol{e} = \begin{bmatrix} e^{p_{\mathrm{t}}} \\ e^{p_{\mathrm{r}}} \\ e^{\varepsilon_{\mathrm{t}}} \\ e^{\varepsilon_{\mathrm{r}}} \end{bmatrix} = \begin{bmatrix} \delta_{p_{\mathrm{t}}} H \\ \delta_{p_{\mathrm{r}}} H \\ \delta_{\varepsilon_{\mathrm{t}}} H \\ \delta_{\varepsilon_{\mathrm{r}}} H \end{bmatrix}. \tag{28}$$

The total energy (we neglect the gravity potential energy and just focus on the quadratic energy functions) becomes the following formulation:

$$\dot{H}_{\mathrm{B}} = \int_0^L \partial_x H \cdot \dot{\boldsymbol{x}} \mathrm{d}z = -\int_0^L \boldsymbol{e}^\top \cdot \boldsymbol{f} \mathrm{d}z. \tag{29}$$

Applying integration by parts on Eq. (29), one obtains

$$\dot{H}_{\mathrm{B}} = (e^{p_{\mathrm{t}}} e^{\varepsilon_{\mathrm{t}}} + e^{p_{\mathrm{r}}} e^{\varepsilon_{\mathrm{r}}})|_0^L. \tag{30}$$

Defining the boundary flow and effort variables as

$$\begin{bmatrix} f_\partial^{\mathrm{t}} \\ f_\partial^{\mathrm{r}} \\ e_\partial^{\mathrm{t}} \\ e_\partial^{\mathrm{r}} \end{bmatrix} = \begin{bmatrix} e^{p_{\mathrm{t}}}|_{\partial Z} \\ e^{p_{\mathrm{r}}}|_{\partial Z} \\ e^{\varepsilon_{\mathrm{t}}}|_{\partial Z} \\ e^{\varepsilon_{\mathrm{r}}}|_{\partial Z} \end{bmatrix}, \tag{31}$$

where $e|_{\partial Z}$denotes the restriction on the border of the domain $Z = [0, L]$. Comparing the right hand sides of (29) and (30), it is clear that the increase of the total energy is equal to the power through the borders. And the power continuity and conservation equation is fulfilled as

$$\int_Z \boldsymbol{e}^\top \cdot \boldsymbol{f} \mathrm{d}z + \left(f_\partial^{\mathrm{t}} \cdot e_\partial^{\mathrm{t}} + f_\partial^{\mathrm{r}} \cdot e_\partial^{\mathrm{r}}\right)\big|_{\partial Z} = 0. \tag{32}$$

Finally, Eq. (27) can be rewrote shortly as

$$-\boldsymbol{f} = \boldsymbol{J}(z)\partial_x H = \boldsymbol{J}(z)\boldsymbol{e}, \tag{33}$$

where $\boldsymbol{J}(z)$ is a skew-symmetric differential operator as that in Eq.(2). Using the definition of flow, effort variables (28) and the system state equations (33), one can define a bilinear geometric structure, a Dirac structure $\mathscr{D}$:

$$\begin{aligned} \mathscr{D} = \{(\boldsymbol{f},\ & f_0^{\mathrm{t}}, f_\partial^{\mathrm{r}}, \boldsymbol{e}, e_\partial^{\mathrm{t}}, e_\partial^{\mathrm{r}}) \in \mathscr{F} \times \mathscr{E} | \\ & -\boldsymbol{f} = \boldsymbol{J}(z)\boldsymbol{e} \text{ and Eq.}(30) \text{ holds } \}. \end{aligned} \tag{34}$$

2.3.3 Structure-preserving Spatial Discretization

In order to solve the distributed parameter model of Timoshenko beam, we need to transfer its Port-Hamiltonian model into a lumped-parameter model. The skew-symmetric differential operator has to be retained in the new discretized model, which means that the discretization method should preserve such certain (geometric or structural) property. In (Moulla et al., 2012), a structure-preserving spatial discretization method is applied to approximate the infinite-dimensional Timoshenko model by the pseudo-spectral method. The discretization of the Port-Hamiltonian system is completed with the finite-dimensional approximation of the energy and the constitutive relations based on the discretization of the (Stokes-) Dirac structure. Furthermore, the boundary port variables are preserved and specified (interconnection) port variables (inputs and outputs) in the resulting lumped Port-Hamiltonian model during the whole process.

The geometric discretization has proven to provide a good approximation of system properties in (Wang et al., 2017), such as the spectrum of the differential operators. Some essential steps are reviewed in this section.

Based on the formulation (27), we rewrote the Dirac structure (34) as

$$-\boldsymbol{f} = \begin{bmatrix} & & 1 & 0 \\ & & 0 & 1 \\ 1 & 0 & & \\ 0 & 1 & & \end{bmatrix} \partial_z \boldsymbol{e} + \begin{bmatrix} & & 0 & 0 \\ & & 1 & 0 \\ 0 & -1 & & \\ 0 & 0 & & \end{bmatrix} \boldsymbol{e}_* \tag{35}$$

so we can classify the effort vectors as $\boldsymbol{e}$ and $\boldsymbol{e}_*$, depending on whether it is subject to differentiation or not.

According to the pseudo-spectral method proposed for canonical systems of two conservation laws, we define different approximation bases for the flows $\boldsymbol{f}^v \in \{\boldsymbol{f}^{p_{\mathrm{t}}}, \boldsymbol{f}^{p_{\mathrm{r}}}, \boldsymbol{f}^{\varepsilon_{\mathrm{t}}}, \boldsymbol{f}^{\varepsilon_{\mathrm{r}}}\}$ and the efforts $\boldsymbol{e}^v \in \{\boldsymbol{e}^{p_{\mathrm{t}}}, \boldsymbol{e}^{p_{\mathrm{r}}}, \boldsymbol{e}^{\varepsilon_{\mathrm{t}}}, \boldsymbol{e}^{\varepsilon_{\mathrm{r}}}\}$.

$$\begin{aligned} &\boldsymbol{f}^v(t,z) \approx \sum_{k=0}^{N-1} f_k^v \varphi_k(z),\ \boldsymbol{e}_*^v(t,z) \approx \sum_{k=0}^{N-1} e_{*,k}^v \varphi_k(z), \\ &\boldsymbol{e}^v(t,z) \approx \sum_{i=0}^{N} e_i^v \phi_i(z). \end{aligned} \tag{36}$$

The time dependent coefficients are collected in the vectors

$$\boldsymbol{f}^v, \boldsymbol{e}_*^v \in \mathbb{R}^N \text{ and } \boldsymbol{e}^v \in \mathbb{R}^{N+1}, v \in \{p_{\mathrm{t}}, p_{\mathrm{r}}, \varepsilon_{\mathrm{t}}, \varepsilon_{\mathrm{r}}\} \tag{37}$$

$\varphi_k(z)$ and $\phi_i(z)$ are the basis functions for flows and efforts, and satisfying the exact differentiation or

compatibility condition (Vu et al., 2013):

$$\begin{aligned} \mathscr{E} &= \operatorname{span}\{\phi_0,\ldots,\phi_N\} \\ \mathscr{F} &= \operatorname{span}\{\varphi_0,\ldots,\varphi_{N-1}\} \\ \partial_x \mathscr{E} &= \mathscr{F}. \end{aligned} \tag{38}$$

Then we chose the interpolation Lagrange polynomials of degree N and $N-1$ as suitable bases functions for the efforts and flows:

$$\varphi_k(z) = \prod_{j=0, j\neq k}^{N-1} \frac{z-z_j}{z_k-z_j}, \phi_i(z) = \prod_{j=0, j\neq i}^{N} \frac{z-\zeta_j}{\zeta_i-\zeta_j}. \tag{39}$$

$z_k \in (0,L), k = 0,\ldots,N-1$ and $\zeta_i \in (0,L)$, $i = 0,\ldots,N$ are the collocation points for $\varphi_k(z)$ and $\phi_i(z)$ respectively. In this paper, we choose the zeros of Legendre polynomials to reduce the Runge's phenomenon (Cardoso-Ribeiro et al., 2016), i.e. the occurrence of numerical oscillations at the boundaries of the interval with increasing number of collocation points.

Denote $\boldsymbol{\phi} = [\phi_0,\ldots,\phi_N]^\top$ the vector of effort basis functions and

$$\boldsymbol{\Phi} = \begin{bmatrix} \boldsymbol{\phi}(0)^\top \\ \boldsymbol{\phi}(L)^\top \end{bmatrix}. \tag{40}$$

Let $\boldsymbol{f}_\partial^{\mathrm{t/r}} = \left[f_0^{\mathrm{t/r}}, f_L^{\mathrm{t/r}}\right]^\top$ and $\boldsymbol{e}_\partial^{\mathrm{t/r}} = \left[e_0^{\mathrm{t/r}}, e_L^{\mathrm{t/r}}\right]^\top$ be the vectors of boundary flows and efforts corresponding to translational or rotational motion. Inserting (36) into (35) and (31), one obtains the linear system of equations

$$\begin{aligned} -\begin{bmatrix} \boldsymbol{f}^{p_\mathrm{t}} \\ \boldsymbol{f}^{p_\mathrm{r}} \\ \boldsymbol{f}^{\varepsilon_\mathrm{t}} \\ \boldsymbol{f}^{\varepsilon_\mathrm{r}} \end{bmatrix} &= \begin{bmatrix} \boldsymbol{D}\,\boldsymbol{0} & & \\ & \boldsymbol{0}\,\boldsymbol{D} & \\ \boldsymbol{D}\,\boldsymbol{0} & & \\ & \boldsymbol{0}\,\boldsymbol{D} & \end{bmatrix} \begin{bmatrix} \boldsymbol{e}^{p_t} \\ \boldsymbol{e}^{p_r} \\ \boldsymbol{e}^{\varepsilon_t} \\ \boldsymbol{e}^{\varepsilon_\mathrm{r}} \end{bmatrix} + \begin{bmatrix} & \boldsymbol{0}\,\boldsymbol{0} & \\ & & \boldsymbol{I}\,\boldsymbol{0} \\ \boldsymbol{0} & -\boldsymbol{I} & \\ 0 & 0 & \end{bmatrix} \begin{bmatrix} \boldsymbol{e}_*^{p_\mathrm{t}} \\ \boldsymbol{e}_*^{p_\mathrm{r}} \\ \boldsymbol{e}_*^{\varepsilon_\mathrm{t}} \\ \boldsymbol{e}_*^{\varepsilon_\mathrm{r}} \end{bmatrix} \\ \begin{bmatrix} \boldsymbol{f}_\partial^{\mathrm{t}} \\ \boldsymbol{f}_\partial^{\mathrm{r}} \\ \boldsymbol{e}_\partial^{\mathrm{t}} \\ \boldsymbol{e}_\partial^{\mathrm{t}} \end{bmatrix} &= \begin{bmatrix} \boldsymbol{\Phi} & & & \\ & \boldsymbol{\Phi} & & \\ & & \boldsymbol{\Phi} & \\ & & & \boldsymbol{\Phi} \end{bmatrix} \begin{bmatrix} \boldsymbol{e}^{p_t} \\ \boldsymbol{e}^{p_r} \\ \boldsymbol{e}^{\varepsilon_t} \\ \boldsymbol{e}^{\varepsilon_\mathrm{r}} \end{bmatrix}. \end{aligned} \tag{41}$$

The elements of the derivative matrix $\boldsymbol{D} \in \mathbb{R}^{N\times(N+1)}$ are obtained from the spatial derivative of the effort bases functions at the flow collocation points:

$$D_{k+1,i+1} = \partial_x \phi_i(z_k), \tag{42}$$

with $i = 0,\ldots,N, k = 0,\ldots,N-1$. In accordance with the distributed parameter model, an additional coupling term with identity matrices $\boldsymbol{I} = \boldsymbol{I}_N$ appears on the right hand side of (42).

Replacing the approximations of flows and efforts in the energy balance, we obtain

$$\dot{H} \approx \sum_{v\in\{p_\mathrm{t},p_\mathrm{r},\varepsilon_\mathrm{t},\varepsilon_\mathrm{r}\}} (\boldsymbol{e}^v)^\top \boldsymbol{M}\boldsymbol{f}^v \tag{43}$$

with the elements of the non-square matrix $\boldsymbol{M} \in \mathbb{R}^{(N+1)\times N}$ defined as

$$M_{i+1,k+1} = \int_0^L \phi_i(z)\varphi_k(z)\mathrm{d}z. \tag{44}$$

The right hand side of (43) consists of degenerated bilinear forms between the vectors of discrete flows and efforts. Due to the degeneracy (the kernel of $\boldsymbol{M}$ is non-empty), this bilinear form does not qualify to define a Dirac structure on the finite-dimensional bond space of reduced flows and efforts $\mathscr{F}_\mathrm{r} \times \mathscr{E}_\mathrm{r}$ with $\left(\boldsymbol{e}^{p_\mathrm{t}}, \boldsymbol{e}^{p_\mathrm{r}}, \boldsymbol{e}^{\varepsilon_\mathrm{t}}, \boldsymbol{e}^{\varepsilon_\mathrm{r}}, \boldsymbol{e}_\partial^{\mathrm{t}}, \boldsymbol{e}_\partial^{\mathrm{r}}\right) \in \mathscr{E}_\mathrm{r} \in \mathbb{R}^{4N+8}$ and $\left(\boldsymbol{f}^{p_\mathrm{t}}, \boldsymbol{f}^{p_\mathrm{r}}, \boldsymbol{f}^{\varepsilon_\mathrm{t}}, \boldsymbol{f}^{\varepsilon_\mathrm{r}}, \boldsymbol{f}_\partial^{\mathrm{t}}, \boldsymbol{f}_\partial^{\mathrm{r}}\right) \in \mathscr{F}_\mathrm{r} \in \mathbb{R}^{4N+4}$. It can, however, be shown that the power continuity equation (32) is approximated via

$$\sum_{v\in\left\{p_\mathrm{t},p_\mathrm{r},\varepsilon_i,\varepsilon_j\right\}} (\boldsymbol{e}^v)^\top \boldsymbol{M}\boldsymbol{f}^v + \sum_{u\in\{\mathrm{t,r}\}} \left(\boldsymbol{e}_\partial^u\right)^\top \boldsymbol{M}\boldsymbol{f}_\partial^u = 0. \tag{45}$$

To obtain a non-degenerate power pairing, vectors of reduced effort variables $\tilde{\boldsymbol{e}}^v \in \mathbb{R}^N$ are defined:

$$\tilde{\boldsymbol{e}}^v = \boldsymbol{M}^\mathrm{T}\boldsymbol{e}^v. \tag{46}$$

These shall be, we discretize the constitutive equation $\boldsymbol{e} = (\delta_x H)^\top$, derived from a discrete energy. Note that $\dot{\boldsymbol{x}} = -\boldsymbol{f}$ holds, i.e. states and flows are discretized with respect to the same basis. We can define $\dot{\boldsymbol{x}}^v = -\boldsymbol{f}^v$ and replace the approximation in $H = \int_Z \mathscr{H}\mathrm{d}z$ with Hamiltonian density. We obtain

$$H \approx \frac{1}{2}\sum_v c^v (\boldsymbol{x}^v)^\top \boldsymbol{S}\boldsymbol{x}^v,\ c^v \in \left\{\frac{1}{\rho}, \frac{1}{I_\rho}, K_s, K_b\right\}, \tag{47}$$

where the elements of $\boldsymbol{S} \in \mathbb{R}^{N\times N}$ are given by

$$S_{i+1,j+1} = \int_0^L \varphi_i(z)\varphi_j(z)\mathrm{d}z. \tag{48}$$

The required discretized constitutive relation is simply

$$\tilde{\boldsymbol{e}}^v = \left(\frac{\partial H}{\partial \boldsymbol{x}^v}\right)^\top = c^v \boldsymbol{S}\boldsymbol{x}^v, \forall v. \tag{49}$$

On the other hand, the relation for the discretized effort vectors $\boldsymbol{e}_*^v$ in the flow (or state) bases becomes

$$\boldsymbol{e}_*^v = c^v \boldsymbol{x}^v = \boldsymbol{S}^{-1}\tilde{\boldsymbol{e}}^v = \boldsymbol{S}^{-1}\boldsymbol{M}^\top \boldsymbol{e}^v. \tag{50}$$

According to (Moulla et al., 2012), the discretised Timoshenko beam can be formulated into an input-/output (I/O) representation:

$$\overline{\boldsymbol{f}} = \begin{bmatrix} 0 & \boldsymbol{J}_{s_1} \\ \boldsymbol{J}_{s_2} & 0 \end{bmatrix} \cdot \overline{\boldsymbol{e}} \tag{51}$$

with

$$\overline{f} = \left[\begin{array}{cccccccc} \boldsymbol{f}^{p_{\mathrm{t}}}, -e^{\mathrm{t}}_{\partial 0}, \boldsymbol{f}^{p_{\mathrm{r}}}, -e^{\mathrm{r}}_{\partial 0}, \boldsymbol{f}^{\varepsilon_{\mathrm{t}}}, f^{\mathrm{t}}_{\partial L}, \boldsymbol{f}^{\varepsilon_{\mathrm{r}}}, f^{\mathrm{r}}_{\partial L} \end{array} \right]^{\top}$$

$$\overline{e} = \left[\tilde{\boldsymbol{e}}^{p_{\mathrm{r}}}, f^{\mathrm{t}}_{\partial 0}, \tilde{\boldsymbol{e}}^{p_{\mathrm{r}}}, f^{\mathrm{r}}_{\partial 0}, \tilde{\boldsymbol{e}}^{\varepsilon_{\mathrm{t}}}, e^{\mathrm{t}}_{\partial L}, \tilde{\boldsymbol{e}}^{\varepsilon_{\mathrm{r}}}, e^{\mathrm{r}}_{\partial L} \right]^{\top}$$

$$\boldsymbol{J}_{s_1} = \begin{bmatrix} \begin{bmatrix} -\boldsymbol{D} \\ -\boldsymbol{\phi}_0^{\top} \end{bmatrix} \begin{bmatrix} \boldsymbol{M}^{\top} \\ \boldsymbol{\phi}_L^{\top} \end{bmatrix}^{-1} & \boldsymbol{0} \\ \begin{bmatrix} -\boldsymbol{S}^{-1}\boldsymbol{M}^{\top} \\ \boldsymbol{0} \end{bmatrix} \begin{bmatrix} \boldsymbol{M}^{\top} \\ \boldsymbol{\phi}_L^{\top} \end{bmatrix}^{-1} & \begin{bmatrix} -\boldsymbol{D} \\ -\boldsymbol{\phi}_0^{\top} \end{bmatrix} \begin{bmatrix} \boldsymbol{M}^{\top} \\ \boldsymbol{\phi}_L^{\top} \end{bmatrix}^{-1} \end{bmatrix}$$

$$\boldsymbol{J}_{s_2} = \begin{bmatrix} \begin{bmatrix} -\boldsymbol{D} \\ -\boldsymbol{\phi}_L^{\top} \end{bmatrix} \begin{bmatrix} \boldsymbol{M}^{\top} \\ \boldsymbol{\phi}_{0^{\top}} \end{bmatrix}^{-1} & \begin{bmatrix} -\boldsymbol{S}^{-1}\boldsymbol{M}^{\top} \\ \boldsymbol{0} \end{bmatrix} \begin{bmatrix} \boldsymbol{M}^{\top} \\ \boldsymbol{\phi}_L^{\top} \end{bmatrix}^{-1} \\ \boldsymbol{0} & \begin{bmatrix} -\boldsymbol{D} \\ -\boldsymbol{\phi}_L^{\top} \end{bmatrix} \begin{bmatrix} \boldsymbol{M}^{\top} \\ \boldsymbol{\phi}_0^{\top} \end{bmatrix}^{-1} \end{bmatrix}$$

Indeed, $\boldsymbol{J}_{s_1} = \boldsymbol{J}_{s_2}^{\top}$, i.e. the interconnection matrix $\boldsymbol{J} \in \mathbb{R}^{(4N+4)\times(4N+4)}$ is skew-symmetric.

We obtain the explicit state space model in linear Port-Hamiltonian form

$$\begin{aligned} \dot{\boldsymbol{X}} &= \boldsymbol{J}_{4N\times 4N}\boldsymbol{Q}_{4N\times 4N}\boldsymbol{X} + \boldsymbol{G}_{4N\times 4}\boldsymbol{U} \\ \boldsymbol{Y} &= \boldsymbol{G}^{\top}_{4N\times 4}\boldsymbol{Q}_{4N\times 4N} + \boldsymbol{D}_{4\times 4}\boldsymbol{U}. \end{aligned} \tag{52}$$

The vector $\boldsymbol{x}^v \in \mathbb{R}^N$ is merged in the overall state vector $\boldsymbol{X} \in \mathbb{R}^{4N}$, $\boldsymbol{Q}_{4N\times 4N} = \text{blockdiag}\left\{\boldsymbol{S}/\rho, \boldsymbol{S}/I_\rho, K_b\boldsymbol{S}, K_s\boldsymbol{S}\right\}$ is the overall energy (Hessian) matrix, and $\boldsymbol{U} \in \mathbb{R}^4$, $\boldsymbol{Y} \in \mathbb{R}^4$ are the vectors of boundary inputs and collocated, power conjugated outputs. They are composed of the elements of the boundary flow an effort vectors. In the terms of the physical boundary variables we have

$$\boldsymbol{U}(t) = \begin{bmatrix} U_1 \\ U_2 \\ U_3 \\ U_4 \end{bmatrix} = \begin{bmatrix} v(0) \\ \omega(0) \\ Q(L) \\ M(L) \end{bmatrix},$$

$$\boldsymbol{Y}(t) = \begin{bmatrix} Y_1 \\ Y_2 \\ Y_3 \\ Y_4 \end{bmatrix} = \begin{bmatrix} -Q(0) \\ -M(0) \\ v(L) \\ \omega(L) \end{bmatrix}.$$

2.4 Port-Hamiltonian Model of the Hydraulic Actuated Telescopic Boom System

2.4.1 Modeling of the Telescopic Boom Structure

Based on the Timoshenko assumption and its Port-Hamiltonian representation, it is not difficult to build a proper mathematical model for the structure of telescopic boom. However there are some modifications should be clarified. The coefficients ρ, I_ρ, I of the new beam model are not constant. Considering the telescopic boom structure, its boom sections are decreasing so that all the other boom sections can be pulled back into the first boom, it means that a homogeneous beam model is no longer suitable. The boom structure will be modeled as a N-stepwise beam with different coefficients for each boom section, a non-homogeneous Timoshenko beam. However, each boom section can be considered as a homogeneous Timoshenko beam and the boundary conditions between each two sections are specified as fixed according to the continuous conditions. The overlapping parts of the boom sections and the telescopic mechanism are neglected in the purpose of simplification.

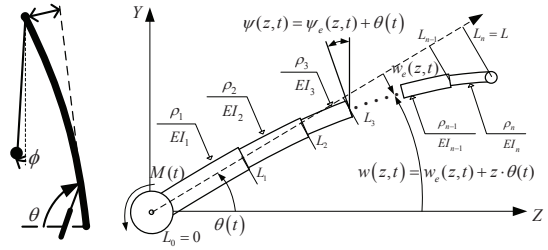

Figure 3: Telescopic boom and its simplified model: the rotating non-homogeneous Timoshenko beam.

According to the definition of power variables (25) and (26), we can define the new power variables for the k^{th} section of the N-stepwise beam in the domain of $D_k := [L_{k-1}, L_k]$ as $p_{\mathrm{t},k}, p_{\mathrm{r},k}, \varepsilon_{\mathrm{t},k}, \varepsilon_{\mathrm{r},k}, k = 1,\ldots,n$. For each part of the stepwise Timoshenko beam, a Dirac structure $\mathscr{D}_k$ can be acquired by using the corresponding power variables.

According to the Port-Hamiltonian form (51), the I/O represent of the kth boom is represented as system Σ_k

$$\Sigma_k : \begin{cases} \dot{\boldsymbol{X}}^k = \boldsymbol{J}^k \left(\dfrac{\partial H^k}{\partial \boldsymbol{x}^k} \right)^{\top} + \boldsymbol{G}^k \boldsymbol{U}^k \\ \boldsymbol{Y}^k = \left(\boldsymbol{G}^k \right)^{\top} \left(\dfrac{\partial H^k}{\partial \boldsymbol{x}^k} \right)^{\top} + \boldsymbol{D}^k \boldsymbol{U}^k \\ \boldsymbol{U}^k = \left[\begin{array}{cccc} v^k_{k-1} & \omega^k_{k-1} & Q^k_k & M^k_k \end{array} \right]^{\top} \\ \boldsymbol{Y}^k = \left[-Q^k_{k-1} - M^k_{k-1} v^k_k \quad \omega^k_k \right]^{\top} \end{cases} \tag{53}$$

the superscripts indicate that the variables are belong to the k^{th} beam and the subscripts represent the connection points.

2.4.2 Interconnection between Subsystem

Now we focus on the interconnection between subsystems. The telescopic boom structure can be considered as the combination of multiple subsystem and each of them is a homogeneous Timoshenko beam. Based on the geometrical and mechanical continuous conditions, the flows and efforts of the k^{th} and

$(k+1)^{\text{th}}$ beam sections through the connection point L_k have the following relations

$$\begin{aligned} f_\partial^{\mathrm{t},k}(L_k,t) &= f_\partial^{\mathrm{t},k+1}(L_k,t) \\ f_\partial^{\mathrm{r,k}}(L_k,t) &= f_\partial^{\mathrm{r},k+1}(L_k,t) \\ e_\partial^{\mathrm{t},k}(L_k,t) &= e_\partial^{\mathrm{t},k+1}(L_n,t) \\ e_\partial^{\mathrm{r},k}(L_k,t) &= e_\partial^{\mathrm{r},k+1}(L_k,t) \end{aligned} \tag{54}$$

which mean that the inputs and outputs of the adjacent two beams have similar relations at the connection point L_k

$$\boldsymbol{Y}_k^k = \boldsymbol{U}_k^{k+1}, \boldsymbol{Y}_k^{k+1} = -\boldsymbol{U}_k^k. \tag{55}$$

According to the I/O representation (53) as Port-Hamiltonian system and the transfer characteristics (55) between outputs and inputs, the boom structure can be built as a series system showed in Fig. 4.

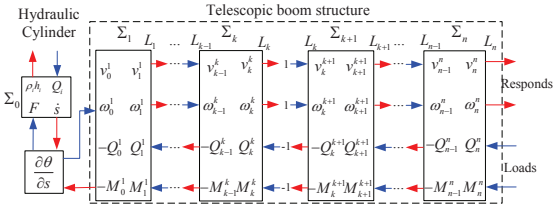

Figure 4: Interconnection of multiple beam and hydraulic system.

The interconnection between the hydraulic system and the boom structure is reflected by the luffing mechanism, in which the hydraulic cylinder acts as the actuator. The output of the hydraulic system, the velocity of the piston, can be transferred to the input angle velocity of the first beam at its boundary $(z=0)$.

Based on the measurements of luffing mechanism (the length of the cylinder and the positions of the joints), the rotation of the boom can be expressed as $\theta(t) = \partial_s\theta \cdot s(t)$, the actuate force and moment have the relation $F = \partial_s \cdot \theta M$. Therefor we have the I/O transfer relation between the hydraulic system and the boom structure as

$$\begin{aligned} U_0^{\mathrm{r},1} &= \omega_0^1 = \partial_s\theta \cdot \dot{s} = \partial_s\theta \cdot y_v \\ u_F &= F(t) = \partial_s\theta \cdot M_0^1 = \partial_s\theta \cdot Y_0^{\mathrm{r},1} \end{aligned} \tag{56}$$

which illustrates the interconnection between the two systems in different domains.

Finally, we have the complete model of the hydraulic actuated telescopic boom system. The load at the boom's tip and the hydraulic flows though the cylinder are the system inputs, the velocity responds at the boom's tip and the enthalpy change of the hydraulic system are the system outputs.

3 SIMULATION AND RESULTS

In order to evaluate the performance of our complete model, we firstly evaluate the approximation quality of the finite-dimensional model of non-homogeneous Timoshenko beam based on the geometric discretization.

We define a stepped beam model with three sets of parameters as Table 1. The model of each part of the beam are built as a Port-Hamiltonian system, discretized and implemented in MATLAB/Simulink individually. Then connect these three I/O representations as a series system. A finite element model using the given parameters (Table 1) is also built in NODYA, a dynamic finite element analysis programme developed by our institute. An eigenvalue analysis is applied firstly to check the frequencies, and the next step is to check the respond behaviors by the dynamic analysis.

Table 1: System parameters.

Parameter	Beam 1	Beam 2	Beam 3
Length		0.3m	
Width	0.02m	0.015	0.01
Depth	0.005m	0.004m	0.003m
Density		7850kg	
Yong's modulus		210GPa	
Poisson's ratio		0.33	
Shear factor		5/6	

The results of eigenvalue analysis is listed in Table 2, the deviations between the two models are less than 4% . It means that the Port-Hamiltonian system representation and the corresponding geometric discretization are still suitable for the non-homogeneous Timoshenko beam.

Table 2: Eigenvalue analysis results.

Mode num.	FE-	PH	Deviation
1	7.37Hz	7.54Hz	2%
2	27.5Hz	28.2Hz	3%
3	65.9Hz	67.9Hz	3%
4	136.4Hz	141Hz	3%

Fig. 5 (b) represents the transient responds of the FE-model and the Port-Hamiltonian model, both have the definition of input ω_0^1 as Fig. 5 (a) shows. The amplitudes of the responding angle velocity at the boom's tip are very close. And the difference of the eigenvalue is also reflected.

Next, we can evaluate the model of complete telescopic boom system using the verified Port-Hamiltonian model of boom structure. The model

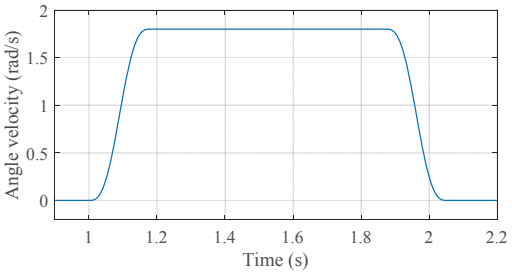

(a) Input angle velocity

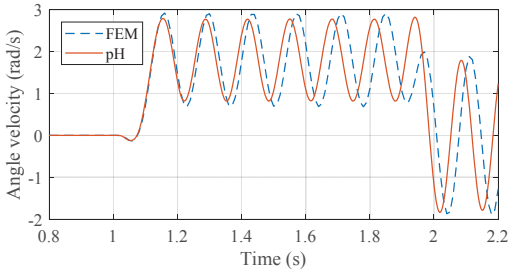

(b) Output angle velocity

Figure 5: Desired input and the transient responds of FE-model and Port-Hamiltonian model.

of the hydraulic system with the parameter set as in Table 3 is also implemented in Matlab/Simulink. Then the model can be easily connected to the model of boom structure by the specified input and output ports.

Table 3: Parameters of hydraulic system.

Parameters	Value
Supply pressure	10bar
Tank pressure	0bar
Piston Area and area ratio	0.0001m^2, 0.75
Bulk modulus	1.2GPa
Piston stoke length	0.25m

In order to avoid the strong nonlinear characteristic of luffing mechanism, we set the limit of the input angle displacement to $\pi/3$. Fig. 6 shows the transient responds of the boom structure model and the complete model including the hydraulic system. In this case, the influence of the hydraulic system is reflected by the respond time delay.

4 CONCLUSION AND OUTLOOK

In this paper, we presented a modeling method and a corresponding discretization method to describe the hydraulic actuated telescopic boom system as a Port-Hamiltonian system. The hydraulic cylinder and tele-

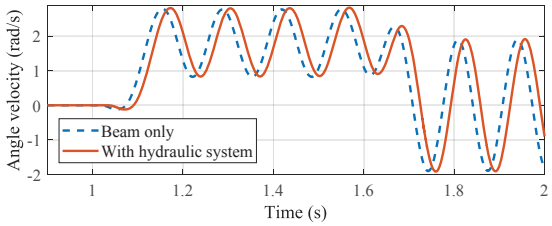

Figure 6: Transient respond of the complete model of telescopic boom, including hydraulic system.

scopic boom structure were modeled in PH formulation respectively. A PH model of non-homogeneous Timoshenko beam is proposed, in order to describe the telescopic boom structure more accurately. The model is proven by the comparison with finite element model. Using the interconnection ports, these individual models could be integrated into a complete model, which include the dynamic behavior of hydraulic system in the dynamic simulation of telescopic boom system. The future works are presented as following:

1. The complete model in this paper is still an open loop system, the vibration responds of the boom structure is not controlled. A closed loop system will be developed. Some suitable controller will be added to the hydraulic system for the purpose of boom vibration suppression.
2. The 2-D bending vibration model of Timoshenko beam is not good enough for the boom structure modeling under some circumstances, especially for the mobile cranes hoisting heavy loads. The boom structure is bearing axial force when the luffing angle is large, in such case the axial deformation cannot be neglected. A more complex beam model will be investigated and its PH formulation will be presented.

ACKNOWLEDGEMENTS

The research is supported by Deutsche Forschungsgemeinschaft (FO 1180 1-1) and National Science Foundation of China (11761131005).

REFERENCES

Cardoso-Ribeiro, F. L., Matignon, D., and Pommier-Budinger, V. (2016). A power-preserving discretization using weak formulation of piezoelectric beam with distributed control ports. *IFAC-PapersOnLine*, 49(8):290–297.

Cheng, L., Ye, Z., and Tong, Z., editors (2016). *Bond graph modeling and simulation analysis of direct drive vol-*

ume control electro-hydraulic servo system with long pipeline. IEEE.

Duindam, V., Macchelli, A., Stramigioli, S., and Bruyninckx, H. (2009). *Modeling and control of complex physical systems: The port-Hamiltonian approach*. Springer Science & Business Media.

Gawthrop, P. J. and Bevan, G. P. (2007). Bond-graph modeling. *IEEE Control Systems Magazine*, 27(2):24–45.

Guo, Y., Liu, D., Yang, S., Li, X., and Chen, J. (2016). Hydraulic–mechanical coupling modeling by bond graph for impact system of a high frequency rock drill drifter with sleeve distributor. *Automation in Construction*, 63:88–99.

Kugi, A. and Kemmetmüller, W. (2004). New energy-based nonlinear controller for hydraulic piston actuators. *European journal of control*, 10(2):163–173.

Macchelli, A. and Melchiorri, C. (2004). Modeling and control of the timoshenko beam. the distributed port hamiltonian approach. *SIAM Journal on Control and Optimization*, 43(2):743–767.

Macchelli, A., Melchiorri, C., and Stramigioli, S. (2009). Port-based modeling and simulation of mechanical systems with rigid and flexible links. *IEEE transactions on robotics*, 25(5):1016–1029.

Moulla, R., Lefevre, L., and Maschke, B. (2012). Pseudo-spectral methods for the spatial symplectic reduction of open systems of conservation laws. *Journal of computational Physics*, 231(4):1272–1292.

Pertsch, A. and Sawodny, O. (2016). Modelling and control of coupled bending and torsional vibrations of an articulated aerial ladder. *Mechatronics*, 33:34–48.

Pertsch, A., Zimmert, N., and Sawodny, O., editors (2009). *Modeling a fire-rescue turntable ladder as piecewise Euler-Bernoulli beam with a tip mass*. IEEE.

Sawodny, O., Aschemann, H., and Bulach, A. (2002). Mechatronical designed control of fire-rescue turntable-ladders as flexible link robots. *IFAC Proceedings Volumes*, 35(1):509–514.

Stadlmayr, R. (2009). *On a combination of feedforward and feedback control for mechatronic systems*. Shaker.

Stadlmayr, R. and Schlacher, K., editors (2004). *Modelling and Control of a Hydraulic Actuated Large Scale Manipulator*, volume 1. Wiley Online Library.

Sun, G. and Kleeberger, M. (2003). Dynamic responses of hydraulic mobile crane with consideration of the drive system. 38(12):1489–1508.

Sun, G., Kleeberger, M., and Liu, J. (2005). Complete dynamic calculation of lattice mobile crane during hoisting motion. *Mechanism and Machine Theory*, 40(4):447–466.

Sun, G. and Liu, J. (2006). Dynamic responses of hydraulic crane during luffing motion. *Mechanism and Machine Theory*, 41(11):1273–1288.

Vu, N. M. T., Lefevre, L., Nouailletas, R., and Brémond, S. (2013). Geometric discretization for a plasma control model. *IFAC Proceedings Volumes*, 46(2):755–760.

Wang, M., Bestler, A., and Kotyczka, P. (2017). Modeling, discretization and motion control of a flexible beam in the port-hamiltonian framework. *IFAC-PapersOnLine*, 50(1):6799–6806.

Zuyev, A. and Sawodny, O. (2005). Stabilization of a flexible manipulator model with passive joints. *IFAC Proceedings Volumes*, 38(1):784–789.